

Figure S1: Time evolution during FRAGMENT-Morocco measurement campaign of 15 min averages of a) the absorption coefficients at 370 nm and 880 nm and the forward scattering at 525 nm, b) the Mass concentration and the particle effective radius, c) the asymmetry parameter and the backscatter fraction (g , BF), and d) the wind speed and fraction velocity (u^*). Between the 4th and the 26th of September the inlet cut-off was of 2.5μ , whereas from the 26th onward the inlet cut-off was of 10μ , as denoted by both the labels and the shadowed background. Periods A, B and C are marked with the orange, yellow and (first) grey shadows.

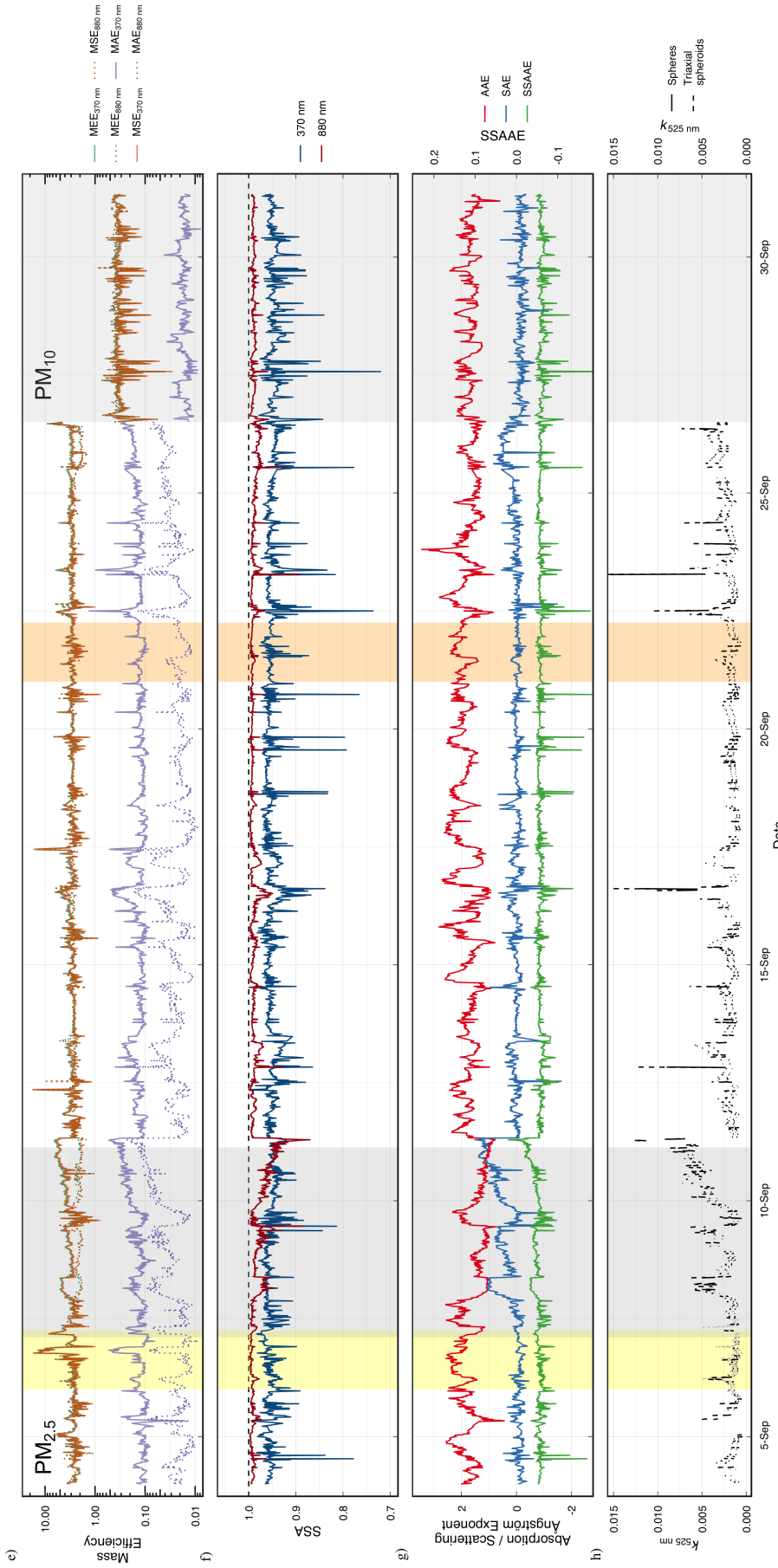


Figure S1: [Continuation:] e) the mass absorption, scattering and extinction efficiency (MAE, MSE, MEE), f) the single scattering albedo (SSA) at both 370 and 880 nm, g) the absorption, scattering and SSA Ångström Exponent (AAE, SAE, MEEAE, SSAAE) and h) the imaginary part of the refractive index for spheres and triaxial spheroids.

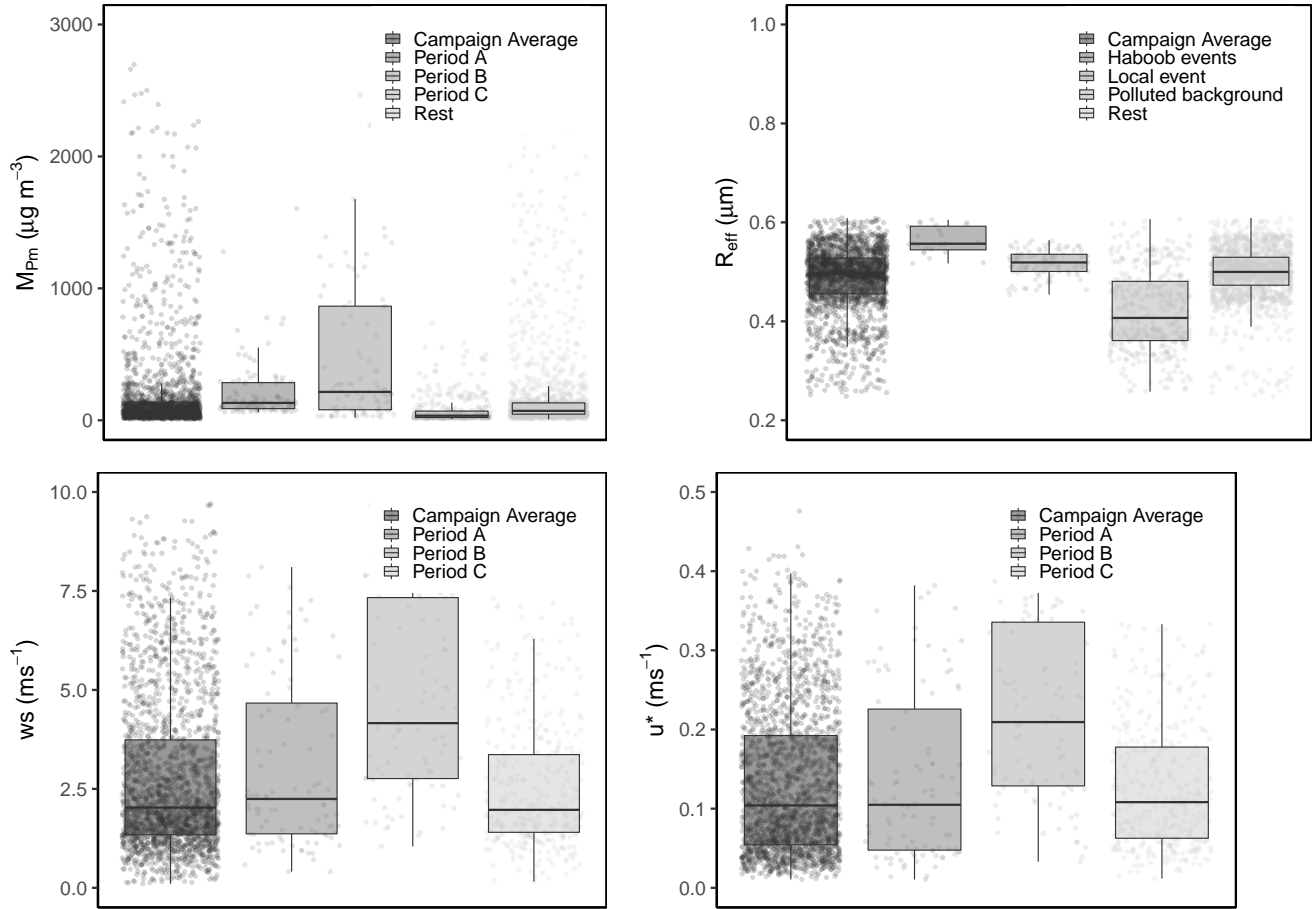


Figure S2: Mass concentration (M_{PM}) and effective radius (R_{eff}) for the selected typical event periods retrieved from the FIDAS particle number size distribution, and the wind speed (ws) and friction velocity (u^*) measured with the 3D windsonic anemometers.

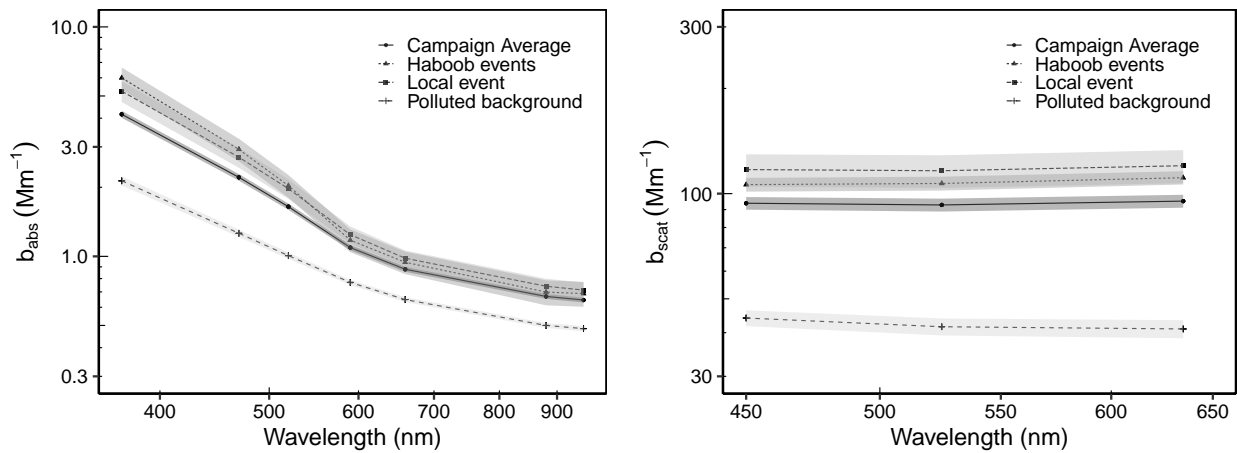


Figure S3: Extensive optical measurements for the selected typical event periods: absorption coefficients (b_{abs}) at the 7 AE33 measuring wavelengths (370, 470, 520, 590, 660, 880, 950 nm), b) scattering coefficients (b_{scat}) at the 3 wavelengths (450, 525, 635 nm) from the polar integrating nephelometer. The points represent the mean, whereas the shaded area represents the standard error.

Figure S4: Mass absorption efficiencies for the selected typical event periods: absorption coefficients (MAE) at the 7 AE33 measuring wavelengths (370, 470, 520, 590, 660, 880, 950 nm), scattering coefficients (MSA) at the 3 wavelengths (450, 525, 635 nm) from the polar integrating nephelometer, and extinction (MEE) at the 7 AE33 measuring wavelengths (370, 470, 520, 590, 660, 880, 950 nm). The points represent the mean, whereas the shaded area represents the standard error.

Figure S5: Single scattering albedo, SSA (upper-left panel), asymmetry parameter, g (upper-right panel), and the backscatter fraction, BF (lower panel), for the selected typical event periods at the 7 AE33 measuring wavelengths (370, 470, 520, 590, 660, 880, 950 nm). The points represent the mean, whereas the shaded area represents the standard error.

Figure S6: Angstrom Exponents for the selected typical event periods for the absorption (AAE), scattering (SAE), and SSA (SSAAE).

Figure S7: Relationship between the particles effective radius (R_e), the wind friction velocity (u) and the absorption (AAE)

Table S1: Average of the imaginary part of the complex refractive index k (multiplied by 10^{-3}) for periods characterized as dust events through-out the PM_{2.5} part of the campaign. The 5th and 95th percentile of the distribution are shown within the parenthesis. Values of k have been obtained for spheres for all the 7 AE33 wavelengths ranging between the near-UV to the near-infrared for all the computed n_r estimates; and the 3 different inlet efficiency cut-off assumptions.

n_r	cut	k: Imaginary refractive index										
		370 nm	470 nm	520 nm	590 nm	660 nm	880 nm	950 nm				
1.48	1.53	2.4 (1.6 3.5)	1.7 (1.0 2.6)	1.4 (0.9 2.3)	1.1 (0.6 1.9)	1.0 (0.5 1.8)	1.0 (0.5 1.8)	1.0 (0.5 1.8)	1.0 (0.5 1.8)	1.0 (0.5 1.8)	1.0 (0.5 1.8)	1.0 (0.5 1.8)
1.48	1.70	2.1 (1.4 3.1)	1.5 (0.9 2.3)	1.3 (0.8 2.0)	1.0 (0.5 1.7)	0.9 (0.5 1.6)	0.9 (0.5 1.6)	0.9 (0.5 1.6)	0.9 (0.5 1.6)	0.9 (0.5 1.6)	0.9 (0.5 1.6)	0.9 (0.5 1.6)
1.48	1.87	1.9 (1.2 2.7)	1.3 (0.8 2.0)	1.1 (0.7 1.8)	0.8 (0.5 1.5)	0.8 (0.4 1.4)	0.8 (0.4 1.4)	0.8 (0.4 1.4)	0.8 (0.4 1.4)	0.8 (0.4 1.4)	0.8 (0.4 1.4)	0.8 (0.4 1.5)
1.49	1.53	2.4 (1.5 3.5)	1.7 (1.0 2.6)	1.4 (0.9 2.3)	1.1 (0.6 1.9)	1.0 (0.5 1.8)	1.0 (0.5 1.8)	1.0 (0.5 1.8)	1.0 (0.5 1.8)	1.0 (0.5 1.8)	1.0 (0.5 1.8)	1.0 (0.5 1.9)
1.49	1.70	2.1 (1.4 3.1)	1.5 (0.9 2.3)	1.3 (0.8 2.0)	0.9 (0.5 1.7)	0.9 (0.5 1.6)	0.9 (0.5 1.6)	0.9 (0.5 1.6)	0.9 (0.5 1.6)	0.9 (0.5 1.6)	0.9 (0.5 1.6)	0.9 (0.4 1.7)
1.49	1.87	1.9 (1.2 2.7)	1.3 (0.8 2.0)	1.1 (0.7 1.8)	0.8 (0.5 1.5)	0.8 (0.4 1.4)	0.8 (0.4 1.4)	0.8 (0.4 1.4)	0.8 (0.4 1.4)	0.8 (0.4 1.4)	0.8 (0.4 1.4)	0.8 (0.4 1.5)
1.50	1.53	2.4 (1.5 3.5)	1.7 (1.0 2.6)	1.4 (0.9 2.3)	1.1 (0.6 1.9)	1.0 (0.5 1.8)	1.0 (0.5 1.8)	1.0 (0.5 1.8)	1.0 (0.5 1.8)	1.0 (0.5 1.8)	1.0 (0.5 1.8)	1.0 (0.5 1.9)
1.50	1.70	2.1 (1.4 3.1)	1.5 (0.9 2.3)	1.2 (0.8 2.0)	0.9 (0.5 1.6)	0.9 (0.4 1.6)	0.9 (0.5 1.6)	0.9 (0.5 1.6)	0.9 (0.5 1.6)	0.9 (0.5 1.6)	0.9 (0.4 1.7)	0.9 (0.4 1.7)
1.50	1.87	1.9 (1.2 2.7)	1.3 (0.8 2.0)	1.1 (0.7 1.8)	0.8 (0.5 1.4)	0.8 (0.4 1.4)	0.8 (0.4 1.4)	0.8 (0.4 1.4)	0.8 (0.4 1.4)	0.8 (0.4 1.4)	0.8 (0.4 1.4)	0.8 (0.4 1.5)
1.51	1.53	2.4 (1.5 3.5)	1.7 (1.0 2.6)	1.4 (0.9 2.3)	1.1 (0.6 1.9)	1.0 (0.5 1.8)	1.0 (0.5 1.8)	1.0 (0.5 1.8)	1.0 (0.5 1.8)	1.0 (0.5 1.8)	1.0 (0.5 1.8)	1.0 (0.5 1.9)
1.51	1.70	2.1 (1.3 3.1)	1.5 (0.9 2.3)	1.2 (0.8 2.0)	0.9 (0.5 1.6)	0.9 (0.4 1.5)	0.9 (0.5 1.6)	0.9 (0.5 1.6)	0.9 (0.5 1.6)	0.9 (0.5 1.6)	0.9 (0.4 1.7)	0.9 (0.4 1.7)
1.51	1.87	1.9 (1.2 2.7)	1.3 (0.8 2.0)	1.1 (0.7 1.8)	0.8 (0.5 1.4)	0.8 (0.4 1.4)	0.8 (0.4 1.4)	0.8 (0.4 1.4)	0.8 (0.4 1.4)	0.8 (0.4 1.4)	0.8 (0.4 1.4)	0.8 (0.4 1.5)
1.52	1.53	2.4 (1.5 3.5)	1.7 (1.0 2.6)	1.4 (0.9 2.3)	1.1 (0.6 1.9)	1.0 (0.5 1.8)	1.0 (0.5 1.8)	1.0 (0.5 1.8)	1.0 (0.5 1.8)	1.0 (0.5 1.8)	1.0 (0.5 1.8)	1.0 (0.5 1.9)
1.52	1.70	2.1 (1.3 3.1)	1.5 (0.9 2.2)	1.2 (0.8 2.0)	0.9 (0.5 1.6)	0.8 (0.4 1.5)	0.8 (0.4 1.5)	0.8 (0.4 1.5)	0.8 (0.4 1.5)	0.8 (0.4 1.5)	0.8 (0.4 1.6)	0.8 (0.4 1.7)
1.52	1.87	1.9 (1.2 2.7)	1.3 (0.8 2.0)	1.1 (0.7 1.8)	0.8 (0.5 1.4)	0.8 (0.4 1.4)	0.8 (0.4 1.4)	0.8 (0.4 1.4)	0.8 (0.4 1.4)	0.8 (0.4 1.4)	0.8 (0.4 1.4)	0.8 (0.4 1.5)
1.53	1.53	2.4 (1.5 3.5)	1.7 (1.0 2.6)	1.4 (0.9 2.3)	1.1 (0.6 1.9)	1.0 (0.5 1.8)	1.0 (0.5 1.8)	1.0 (0.5 1.8)	1.0 (0.5 1.8)	1.0 (0.5 1.8)	1.0 (0.5 1.8)	1.0 (0.5 1.8)
1.53	1.70	2.1 (1.3 3.0)	1.5 (0.9 2.2)	1.2 (0.7 2.0)	0.9 (0.5 1.6)	0.8 (0.4 1.5)	0.8 (0.4 1.5)	0.8 (0.4 1.5)	0.8 (0.4 1.5)	0.8 (0.4 1.5)	0.8 (0.4 1.5)	0.8 (0.4 1.6)
1.53	1.87	1.9 (1.2 2.7)	1.3 (0.8 2.0)	1.1 (0.7 1.8)	0.8 (0.4 1.4)	0.7 (0.4 1.3)	0.8 (0.4 1.3)	0.8 (0.4 1.3)	0.8 (0.4 1.3)	0.8 (0.4 1.3)	0.8 (0.4 1.4)	0.8 (0.4 1.5)
1.54	1.53	2.4 (1.5 3.5)	1.7 (1.0 2.6)	1.4 (0.8 2.3)	1.0 (0.6 1.8)	1.0 (0.5 1.7)	1.0 (0.5 1.7)	1.0 (0.5 1.7)	1.0 (0.5 1.7)	1.0 (0.5 1.7)	1.0 (0.5 1.7)	1.0 (0.5 1.8)
1.54	1.70	2.1 (1.3 3.0)	1.5 (0.9 2.2)	1.2 (0.7 2.0)	0.9 (0.5 1.6)	0.8 (0.4 1.5)	0.8 (0.4 1.5)	0.8 (0.4 1.5)	0.8 (0.4 1.5)	0.8 (0.4 1.5)	0.8 (0.4 1.5)	0.8 (0.4 1.6)
1.54	1.87	1.8 (1.2 2.7)	1.3 (0.8 2.0)	1.1 (0.7 1.7)	0.8 (0.4 1.4)	0.7 (0.4 1.3)	0.8 (0.4 1.3)	0.8 (0.4 1.3)	0.8 (0.4 1.3)	0.8 (0.4 1.3)	0.8 (0.4 1.4)	0.8 (0.4 1.5)
1.55	1.53	2.4 (1.5 3.5)	1.7 (1.0 2.5)	1.4 (0.8 2.3)	1.0 (0.6 1.8)	0.9 (0.5 1.7)	0.9 (0.5 1.7)	0.9 (0.5 1.7)	0.9 (0.5 1.7)	0.9 (0.5 1.7)	0.9 (0.5 1.7)	0.9 (0.5 1.8)
1.55	1.70	2.1 (1.3 3.0)	1.4 (0.9 2.2)	1.2 (0.7 2.0)	0.9 (0.5 1.6)	0.8 (0.4 1.5)	0.8 (0.4 1.5)	0.8 (0.4 1.5)	0.8 (0.4 1.5)	0.8 (0.4 1.5)	0.8 (0.4 1.5)	0.8 (0.4 1.6)
1.55	1.87	1.8 (1.2 2.7)	1.3 (0.8 2.0)	1.1 (0.67 1.7)	0.8 (0.4 1.4)	0.7 (0.4 1.3)	0.8 (0.4 1.3)	0.8 (0.4 1.3)	0.8 (0.4 1.3)	0.8 (0.4 1.3)	0.8 (0.4 1.4)	0.8 (0.4 1.5)

Table S2: Average of the imaginary part of the complex refractive index k (multiplied by 10^{-3}) for periods characterized as dust events through-out the PM_{2.5} part of the campaign. The 5th and 95th percentile of the distribution are shown within the parenthesis. Values of k have been obtained for biaxial spheroids for all the 7 AE33 wavelengths ranging between the near-UV to the near-infrared for all the computed n_r estimates; and the 3 different inlet efficiency cut-off assumptions.

n_r	cut	k: Imaginary refractive index										
		370 nm	470 nm	520 nm	590 nm	660 nm	880 nm	950 nm				
1.48	1.53	2.5 (1.6 3.6)	1.8 (1.1 2.7)	1.5 (0.9 2.4)	1.1 (0.6 1.9)	1.0 (0.5 1.8)	1.0 (0.5 1.8)	1.0 (0.5 1.8)	1.0 (0.5 1.8)	1.0 (0.5 1.8)	1.0 (0.5 1.8)	1.0 (0.5 1.9)
1.48	1.70	2.1 (1.4 3.1)	1.5 (1.0 2.3)	1.3 (0.8 2.1)	1.0 (0.6 1.7)	0.9 (0.5 1.6)	0.9 (0.5 1.6)	0.9 (0.5 1.6)	0.9 (0.5 1.6)	0.9 (0.5 1.6)	0.9 (0.5 1.6)	0.9 (0.4 1.7)
1.48	1.87	1.9 (1.2 2.8)	1.4 (0.9 2.0)	1.1 (0.7 1.8)	0.9 (0.5 1.5)	0.8 (0.4 1.4)	0.8 (0.4 1.4)	0.8 (0.4 1.4)	0.8 (0.4 1.4)	0.8 (0.4 1.4)	0.8 (0.4 1.5)	0.8 (0.4 1.6)
1.49	1.53	2.4 (1.6 3.5)	1.7 (1.1 2.7)	1.5 (0.9 2.3)	1.1 (0.6 1.9)	1.0 (0.5 1.8)	1.0 (0.5 1.8)	1.0 (0.5 1.8)	1.0 (0.5 1.8)	1.0 (0.5 1.8)	1.0 (0.5 1.8)	1.0 (0.5 1.9)
1.49	1.70	2.1 (1.4 3.1)	1.5 (1.0 2.3)	1.3 (0.8 2.0)	1.0 (0.5 1.7)	0.9 (0.5 1.6)	0.9 (0.5 1.6)	0.9 (0.5 1.6)	0.9 (0.5 1.6)	0.9 (0.5 1.6)	0.9 (0.5 1.6)	0.9 (0.4 1.7)
1.49	1.87	1.9 (1.2 2.7)	1.3 (0.8 2.0)	1.1 (0.7 1.8)	0.9 (0.5 1.5)	0.8 (0.4 1.4)	0.8 (0.4 1.4)	0.8 (0.4 1.4)	0.8 (0.4 1.4)	0.8 (0.4 1.4)	0.8 (0.4 1.5)	0.8 (0.4 1.6)
1.50	1.53	2.4 (1.6 3.5)	1.7 (1.1 2.6)	1.4 (0.9 2.3)	1.1 (0.6 1.9)	1.0 (0.5 1.8)	1.0 (0.5 1.8)	1.0 (0.5 1.8)	1.0 (0.5 1.8)	1.0 (0.5 1.8)	1.0 (0.5 1.8)	1.0 (0.5 1.9)
1.50	1.70	2.1 (1.4 3.1)	1.5 (0.9 2.3)	1.3 (0.8 2.0)	1.0 (0.5 1.7)	0.9 (0.5 1.6)	0.9 (0.5 1.6)	0.9 (0.5 1.6)	0.9 (0.5 1.6)	0.9 (0.5 1.6)	0.9 (0.5 1.6)	0.9 (0.4 1.7)
1.50	1.87	1.9 (1.2 2.7)	1.3 (0.8 2.0)	1.1 (0.7 1.8)	0.8 (0.5 1.5)	0.8 (0.4 1.4)	0.8 (0.4 1.4)	0.8 (0.4 1.4)	0.8 (0.4 1.4)	0.8 (0.4 1.4)	0.8 (0.4 1.4)	0.8 (0.4 1.5)
1.51	1.53	2.4 (1.5 3.5)	1.7 (1.1 2.6)	1.4 (0.9 2.3)	1.1 (0.6 1.9)	1.0 (0.5 1.8)	1.0 (0.5 1.8)	1.0 (0.5 1.8)	1.0 (0.5 1.8)	1.0 (0.5 1.8)	1.0 (0.5 1.8)	1.0 (0.5 1.9)
1.51	1.70	2.1 (1.3 3.1)	1.5 (0.9 2.3)	1.3 (0.8 2.0)	1.0 (0.5 1.7)	0.9 (0.5 1.6)	0.9 (0.5 1.6)	0.9 (0.5 1.6)	0.9 (0.5 1.6)	0.9 (0.5 1.6)	0.9 (0.5 1.6)	0.9 (0.4 1.7)
1.51	1.87	1.9 (1.2 2.7)	1.3 (0.8 2.0)	1.1 (0.7 1.8)	0.8 (0.5 1.5)	0.8 (0.4 1.4)	0.8 (0.4 1.4)	0.8 (0.4 1.4)	0.8 (0.4 1.4)	0.8 (0.4 1.4)	0.8 (0.4 1.4)	0.8 (0.4 1.5)
1.52	1.53	2.4 (1.5 3.5)	1.7 (1.1 2.6)	1.4 (0.9 2.3)	1.1 (0.6 1.9)	1.0 (0.5 1.8)	1.0 (0.5 1.8)	1.0 (0.5 1.8)	1.0 (0.5 1.8)	1.0 (0.5 1.8)	1.0 (0.5 1.8)	1.0 (0.5 1.9)
1.52	1.70	2.1 (1.3 3.0)	1.5 (0.9 2.3)	1.2 (0.8 2.0)	0.9 (0.5 1.6)	0.9 (0.5 1.6)	0.9 (0.5 1.6)	0.9 (0.5 1.6)	0.9 (0.5 1.6)	0.9 (0.5 1.6)	0.9 (0.5 1.6)	0.9 (0.4 1.7)
1.52	1.87	1.9 (1.2 2.7)	1.3 (0.8 2.0)	1.1 (0.7 1.8)	0.8 (0.5 1.4)	0.8 (0.4 1.4)	0.8 (0.4 1.4)	0.8 (0.4 1.4)	0.8 (0.4 1.4)	0.8 (0.4 1.4)	0.8 (0.4 1.4)	0.8 (0.4 1.5)
1.53	1.53	2.4 (1.5 3.5)	1.7 (1.1 2.6)	1.4 (0.9 2.3)	1.1 (0.6 1.9)	1.0 (0.5 1.8)	1.0 (0.5 1.8)	1.0 (0.5 1.8)	1.0 (0.5 1.8)	1.0 (0.5 1.8)	1.0 (0.5 1.8)	1.0 (0.5 1.9)
1.53	1.70	2.1 (1.3 3.0)	1.5 (0.9 2.3)	1.2 (0.8 2.0)	0.9 (0.5 1.6)	0.9 (0.4 1.6)	0.9 (0.4 1.6)	0.9 (0.4 1.6)	0.9 (0.4 1.6)	0.9 (0.4 1.6)	0.9 (0.4 1.6)	0.9 (0.4 1.7)
1.53	1.87	1.9 (1.2 2.7)	1.3 (0.8 2.0)	1.1 (0.7 1.8)	0.8 (0.5 1.4)	0.8 (0.4 1.4)	0.8 (0.4 1.4)	0.8 (0.4 1.4)	0.8 (0.4 1.4)	0.8 (0.4 1.4)	0.8 (0.4 1.4)	0.8 (0.4 1.5)
1.54	1.53	2.4 (1.5 3.5)	1.7 (1.0 2.6)	1.4 (0.9 2.3)	1.1 (0.6 1.9)	1.0 (0.5 1.8)	1.0 (0.5 1.8)	1.0 (0.5 1.8)	1.0 (0.5 1.8)	1.0 (0.5 1.8)	1.0 (0.5 1.8)	1.0 (0.5 1.9)
1.54	1.70	2.1 (1.3 3.0)	1.5 (0.9 2.2)	1.2 (0.8 2.0)	0.9 (0.5 1.6)	0.9 (0.4 1.5)	0.9 (0.4 1.5)	0.9 (0.4 1.5)	0.9 (0.4 1.5)	0.9 (0.4 1.5)	0.9 (0.4 1.5)	0.9 (0.4 1.7)
1.54	1.87	1.8 (1.2 2.7)	1.3 (0.8 2.0)	1.1 (0.7 1.7)	0.8 (0.5 1.4)	0.8 (0.4 1.4)	0.8 (0.4 1.4)	0.8 (0.4 1.4)	0.8 (0.4 1.4)	0.8 (0.4 1.4)	0.8 (0.4 1.4)	0.8 (0.4 1.5)
1.55	1.53	2.4 (1.5 3.5)	1.7 (1.0 2.6)	1.4 (0.8 2.3)	1.1 (0.6 1.8)	1.0 (0.5 1.8)	1.0 (0.5 1.8)	1.0 (0.5 1.8)	1.0 (0.5 1.8)	1.0 (0.5 1.8)	1.0 (0.5 1.8)	1.0 (0.5 1.9)
1.55	1.70	2.1 (1.3 3.0)	1.5 (0.9 2.2)	1.2 (0.7 2.0)	0.9 (0.5 1.6)	0.8 (0.4 1.5)	0.8 (0.4 1.5)	0.8 (0.4 1.5)	0.8 (0.4 1.5)	0.8 (0.4 1.5)	0.8 (0.4 1.5)	0.8 (0.4 1.7)
1.55	1.87	1.8 (1.2 2.7)	1.3 (0.8 2.0)	1.1 (0.7 1.7)	0.8 (0.4 1.4)	0.7 (0.4 1.3)	0.7 (0.4 1.3)	0.7 (0.4 1.3)	0.7 (0.4 1.3)	0.7 (0.4 1.3)	0.7 (0.4 1.3)	0.7 (0.4 1.5)

Table S3: Average of the imaginary part of the complex refractive index k (multiplied by 10^{-3}) for periods characterized as dust events through-out the PM_{2.5} part of the campaign. The 5th and 95th percentile of the distribution are shown within the parenthesis. Values of k have been obtained for triaxial spheroids for all the 7 AE33 wavelengths ranging between the near-UV to the near-infrared for all the computed n_r estimates; and the 3 different inlet efficiency cut-off assumptions.

n_r	cut	k: Imaginary refractive index										
		370 nm	470 nm	520 nm	590 nm	660 nm	880 nm	950 nm				
1.48	1.53	3.8 (2.5 5.4)	2.6 (1.7 3.8)	2.1 (1.3 3.3)	1.5 (0.9 2.6)	1.3 (0.7 2.3)	1.2 (0.6 2.1)	1.1 (0.5 2.1)				
1.48	1.70	3.4 (2.2 4.7)	2.3 (1.5 3.4)	1.8 (1.1 2.9)	1.3 (0.8 2.3)	1.1 (0.6 2.1)	1.1 (0.6 1.9)	1.0 (0.5 1.9)				
1.48	1.87	3.0 (2.0 4.2)	2.0 (1.3 3.0)	1.6 (1.0 2.6)	1.2 (0.7 2.0)	1.0 (0.5 1.8)	1.0 (0.5 1.7)	0.9 (0.4 1.8)				
1.49	1.53	3.8 (2.5 5.4)	2.6 (1.7 3.8)	2.1 (1.3 3.3)	1.5 (0.9 2.6)	1.3 (0.7 2.3)	1.2 (0.6 2.1)	1.1 (0.6 2.1)				
1.49	1.70	3.3 (2.2 4.7)	2.3 (1.5 3.4)	1.8 (1.1 2.9)	1.3 (0.8 2.3)	1.2 (0.6 2.1)	1.1 (0.6 1.9)	1.0 (0.5 1.9)				
1.49	1.87	3.0 (2.0 4.2)	2.0 (1.3 3.0)	1.6 (1.0 2.6)	1.2 (0.7 2.0)	1.0 (0.5 1.9)	1.0 (0.5 1.7)	0.9 (0.4 1.8)				
1.50	1.53	3.8 (2.5 5.4)	2.6 (1.7 3.8)	2.1 (1.3 3.3)	1.5 (0.9 2.6)	1.3 (0.7 2.4)	1.2 (0.6 2.1)	1.1 (0.6 2.1)				
1.50	1.70	3.3 (2.2 4.7)	2.3 (1.5 3.4)	1.9 (1.1 2.9)	1.3 (0.8 2.3)	1.2 (0.6 2.1)	1.1 (0.6 1.9)	1.0 (0.5 1.9)				
1.50	1.87	3.0 (2.0 4.2)	2.0 (1.3 3.0)	1.6 (1.0 2.6)	1.2 (0.7 2.1)	1.0 (0.5 1.9)	1.0 (0.5 1.7)	0.9 (0.4 1.8)				
1.51	1.53	3.7 (2.5 5.3)	2.6 (1.7 3.8)	2.1 (1.3 3.3)	1.5 (0.9 2.6)	1.3 (0.7 2.4)	1.2 (0.6 2.1)	1.1 (0.6 2.1)				
1.51	1.70	3.3 (2.2 4.7)	2.3 (1.4 3.4)	1.8 (1.1 2.9)	1.3 (0.8 2.3)	1.2 (0.6 2.1)	1.1 (0.6 1.9)	1.0 (0.5 2.0)				
1.51	1.87	3.0 (1.9 4.2)	2.0 (1.3 3.0)	1.6 (1.0 2.6)	1.2 (0.7 2.1)	1.0 (0.5 1.9)	1.0 (0.5 1.7)	0.9 (0.4 1.8)				
1.52	1.53	3.7 (2.5 5.3)	2.6 (1.6 3.8)	2.1 (1.3 3.3)	1.5 (0.9 2.6)	1.3 (0.7 2.4)	1.2 (0.6 2.1)	1.1 (0.6 2.1)				
1.52	1.70	3.3 (2.2 4.6)	2.3 (1.4 3.4)	1.8 (1.1 2.9)	1.3 (0.7 2.3)	1.2 (0.6 2.1)	1.1 (0.6 1.9)	1.0 (0.5 2.0)				
1.52	1.87	2.9 (1.9 4.1)	2.0 (1.3 3.0)	1.6 (1.0 2.6)	1.2 (0.7 2.0)	1.0 (0.5 1.9)	1.0 (0.5 1.7)	0.9 (0.4 1.8)				
1.53	1.53	3.7 (2.4 5.2)	2.6 (1.6 3.8)	2.1 (1.3 3.3)	1.5 (0.9 2.6)	1.3 (0.7 2.4)	1.2 (0.6 2.1)	1.1 (0.6 2.2)				
1.53	1.70	3.3 (2.2 4.6)	2.3 (1.4 3.4)	1.8 (1.1 2.9)	1.3 (0.7 2.3)	1.2 (0.6 2.1)	1.1 (0.6 1.9)	1.0 (0.5 2.0)				
1.53	1.87	2.9 (1.9 4.1)	2.0 (1.2 3.0)	1.6 (1.0 2.6)	1.2 (0.7 2.0)	1.0 (0.5 1.9)	1.0 (0.5 1.7)	0.9 (0.4 1.8)				
1.54	1.53	3.7 (2.4 5.2)	2.6 (1.6 3.8)	2.1 (1.3 3.3)	1.5 (0.9 2.6)	1.3 (0.7 2.4)	1.2 (0.6 2.1)	1.1 (0.6 2.2)				
1.54	1.70	3.3 (2.1 4.6)	2.3 (1.4 3.4)	1.8 (1.1 2.9)	1.3 (0.7 2.3)	1.2 (0.6 2.1)	1.1 (0.6 1.9)	1.0 (0.5 2.0)				
1.54	1.87	2.9 (1.9 4.1)	2.0 (1.2 3.0)	1.6 (1.0 2.6)	1.2 (0.7 2.0)	1.0 (0.5 1.9)	1.0 (0.5 1.7)	0.9 (0.4 1.8)				
1.55	1.53	3.7 (2.4 5.2)	2.6 (1.6 3.8)	2.1 (1.3 3.3)	1.5 (0.8 2.6)	1.3 (0.7 2.4)	1.2 (0.6 2.1)	1.1 (0.6 2.2)				
1.55	1.70	3.2 (2.1 4.6)	2.3 (1.4 3.4)	1.8 (1.1 2.9)	1.3 (0.7 2.3)	1.2 (0.6 2.1)	1.1 (0.6 1.9)	1.0 (0.5 2.0)				
1.55	1.87	2.9 (1.9 4.1)	2.0 (1.2 3.0)	1.6 (1.0 2.6)	1.2 (0.6 2.0)	1.0 (0.5 1.9)	1.0 (0.5 1.7)	0.9 (0.4 1.8)				

Table S4: Average of the imaginary part of the complex refractive index k (multiplied by 10^{-3}) for periods characterized as dust events throughout the PM_{2.5} part of the campaign. The 5th and 95th percentile of the distribution are shown within the parenthesis. Values of k have been obtained for the average of the A to F irregular shapes from Gasteiger and Weigner (2018) for all the 7 AE33 wavelengths ranging between the near-UV to the near-infrared for all the computed n_r estimates; and the 3 different inlet efficiency cut-off assumptions.

n_r	cut	k: Imaginary refractive index										
		370 nm	470 nm	520 nm	590 nm	660 nm	880 nm	950 nm				
1.48	1.53	3.0 (1.9 4.6)	2.2 (1.4 3.4)	1.8 (1.1 3.0)	1.4 (0.8 2.4)	1.2 (0.7 2.2)	1.2 (0.6 2.1)	1.1 (0.6 2.1)				
1.48	1.70	2.7 (1.7 4.1)	1.9 (1.2 3.0)	1.6 (1.0 2.7)	1.2 (0.7 2.1)	1.1 (0.6 2.0)	1.1 (0.6 1.9)	1.1 (0.5 2.0)				
1.48	1.87	2.4 (1.6 3.8)	1.8 (1.1 2.8)	1.5 (0.9 2.4)	1.1 (0.6 1.9)	1.0 (0.5 1.8)	1.0 (0.5 1.8)	1.0 (0.5 1.9)				
1.49	1.53	3.0 (1.9 4.5)	2.2 (1.3 3.4)	1.8 (1.1 3.0)	1.4 (0.8 2.4)	1.2 (0.7 2.2)	1.2 (0.6 2.1)	1.1 (0.6 2.1)				
1.49	1.70	2.7 (1.7 4.1)	1.9 (1.2 3.0)	1.6 (1.0 2.7)	1.2 (0.7 2.1)	1.1 (0.6 2.0)	1.1 (0.6 1.9)	1.1 (0.5 2.0)				
1.49	1.87	2.4 (1.6 3.7)	1.8 (1.1 2.7)	1.5 (0.9 2.4)	1.1 (0.6 1.9)	1.0 (0.5 1.8)	1.0 (0.5 1.8)	1.0 (0.5 1.9)				
1.50	1.53	3.0 (1.9 4.5)	2.1 (1.3 3.4)	1.8 (1.1 3.0)	1.4 (0.8 2.4)	1.2 (0.7 2.2)	1.2 (0.6 2.1)	1.1 (0.6 2.2)				
1.50	1.70	2.7 (1.7 4.0)	1.9 (1.2 3.0)	1.6 (1.0 2.7)	1.2 (0.7 2.1)	1.1 (0.6 2.0)	1.1 (0.6 1.9)	1.1 (0.5 2.0)				
1.50	1.87	2.4 (1.5 3.7)	1.7 (1.1 2.7)	1.5 (0.9 2.4)	1.1 (0.6 1.9)	1.0 (0.5 1.8)	1.0 (0.5 1.8)	1.0 (0.5 1.9)				
1.51	1.53	2.9 (1.8 4.5)	2.1 (1.3 3.3)	1.8 (1.1 2.9)	1.4 (0.8 2.4)	1.2 (0.7 2.2)	1.2 (0.6 2.1)	1.2 (0.6 2.2)				
1.51	1.70	2.6 (1.7 4.0)	1.9 (1.2 3.0)	1.6 (1.0 2.6)	1.2 (0.7 2.1)	1.1 (0.6 2.0)	1.1 (0.6 1.9)	1.1 (0.5 2.0)				
1.51	1.87	2.4 (1.5 3.7)	1.7 (1.1 2.7)	1.5 (0.9 2.4)	1.1 (0.6 1.9)	1.0 (0.5 1.8)	1.0 (0.5 1.8)	1.0 (0.5 1.9)				
1.52	1.53	2.9 (1.8 4.4)	2.1 (1.3 3.3)	1.8 (1.1 2.9)	1.3 (0.8 2.4)	1.2 (0.6 2.2)	1.2 (0.6 2.1)	1.2 (0.6 2.2)				
1.52	1.70	2.6 (1.7 4.0)	1.9 (1.2 3.0)	1.6 (1.0 2.6)	1.2 (0.7 2.1)	1.1 (0.6 2.0)	1.1 (0.6 1.9)	1.1 (0.5 2.0)				
1.52	1.87	2.3 (1.5 3.6)	1.7 (1.1 2.7)	1.4 (0.9 2.4)	1.1 (0.6 1.9)	1.0 (0.5 1.8)	1.0 (0.5 1.8)	1.0 (0.5 1.9)				
1.53	1.53	2.9 (1.8 4.4)	2.1 (1.3 3.3)	1.8 (1.1 2.9)	1.3 (0.8 2.3)	1.2 (0.6 2.2)	1.2 (0.6 2.1)	1.2 (0.6 2.2)				
1.53	1.70	2.6 (1.6 4.0)	1.9 (1.2 3.0)	1.6 (1.0 2.6)	1.2 (0.7 2.1)	1.1 (0.6 2.0)	1.1 (0.6 1.9)	1.1 (0.5 2.0)				
1.53	1.87	2.3 (1.5 3.6)	1.7 (1.0 2.7)	1.4 (0.9 2.4)	1.1 (0.6 1.9)	1.0 (0.5 1.8)	1.0 (0.5 1.8)	1.0 (0.5 1.9)				
1.54	1.53	2.9 (1.8 4.4)	2.1 (1.3 3.3)	1.7 (1.1 2.9)	1.3 (0.7 2.3)	1.2 (0.6 2.2)	1.2 (0.6 2.1)	1.2 (0.6 2.2)				
1.54	1.70	2.6 (1.6 3.9)	1.9 (1.1 2.9)	1.6 (0.9 2.6)	1.2 (0.7 2.1)	1.1 (0.6 2.0)	1.1 (0.6 1.9)	1.1 (0.5 2.0)				
1.54	1.87	2.3 (1.5 3.6)	1.7 (1.0 2.7)	1.4 (0.9 2.3)	1.1 (0.6 1.9)	1.0 (0.5 1.8)	1.0 (0.5 1.8)	1.0 (0.5 1.9)				
1.55	1.53	2.8 (1.8 4.3)	2.1 (1.3 3.3)	1.7 (1.0 2.9)	1.3 (0.7 2.3)	1.2 (0.6 2.2)	1.2 (0.6 2.1)	1.2 (0.6 2.2)				
1.55	1.70	2.5 (1.6 3.9)	1.8 (1.1 2.9)	1.6 (0.9 2.6)	1.2 (0.7 2.1)	1.1 (0.6 1.9)	1.1 (0.6 1.9)	1.1 (0.5 2.0)				
1.55	1.87	2.3 (1.5 3.6)	1.7 (1.0 2.6)	1.4 (0.8 2.3)	1.1 (0.6 1.9)	1.0 (0.5 1.8)	1.0 (0.5 1.8)	1.0 (0.5 1.9)				

Figure S8: Retrieved k as in Fig. 7 for a) the retrieval of the averages, and b) the average of the retrievals.

